

## Direct and inverse kinematic model of the OMNI PHANToM

### Modelo cinemático directo e inverso del OMNI PHANToM

GUDIÑO-LAU, Jorge<sup>†</sup>, CHÁVEZ-MONTEJANO, Fidel\*, ALCALÁ, Janeth and CHARRE-IBARRA, Saida

*Universidad de Colima, Facultad de Ingeniería Electromecánica, Km. 20.5 Carretera Manzanillo-Barra de Navidad, C.P. 28869, Manzanillo, Colima, México.*

ID 1° Author: *Jorge, Gudiño-Lau*: **ORC ID:** 0000-0002-0585-908X, **Researcher ID Thomson:** Q-6844-2018, **arXiv ID:** jorgeglau, **PubMed ID:** jorgeglau, **CVU CONACYT ID:** 122644

ID 1° Coauthor: *Fidel, Chávez-Montejano*: **ORC ID:** 0000-0001-6136-69954

ID 2° Coauthor: *Janeth, Alcalá*: **ORC ID:** 0000-0002-0238-3952

ID 3° Coauthor: *Saida, Charre-Ibarra*: **ORC ID:** 0000-0002-3823-5388, **Researcher ID Thomson:** Q-6851-2018

Received: October 09, 2018; Accepted: November 30, 2018

#### Abstract

In this work we describe the kinematic and inverse model of an Omni Phantom haptic device with three degrees of freedom. For direct kinematic analysis the Denavit-Hartenberg methodology is used since it is an open chain robot, and for the inverse kinematics the geometric method is used, since the solution is not trivial. The mathematical analysis to obtain the kinematic model of the haptic device is validated in SolidWorks, Matlab® and experimentally.

#### Haptic device, denavit-hartenberg method, direct and inverse kinematics

#### Resumen

En este trabajo se describe el modelo cinemático e inverso de un dispositivo háptico Omni Phantom de tres grados de libertad. Para el análisis cinemático directo se emplea la metodología Denavit-Hartenberg ya que es un robot de cadenas abierta, y para la cinemática inversa se emplea el método geométrico, ya que la solución no es trivial. El análisis matemático para obtener el modelo cinemático del dispositivo háptico es validado en SolidWorks, Matlab® y experimentalmente.

#### Dispositivo háptico, Metodo denavit-hartenberg, cinemática directa e inversa

**Citation:** GUDIÑO-LAU, Jorge, CHÁVEZ-MONTEJANO, Fidel, ALCALÁ, Janeth, CHARRE-IBARRA, Saida. Direct and inverse kinematic model of the OMNI PHANToM. 2018. 5-9: 25-32.

\* Correspondence to Author (email: fidel\_chavez@uclm.mx)

† Researcher contributing as first author.

## Introduction

The beginnings of robotics are given by the year 1801 when Joseph Jacquard invents a programmable textile machine using punched cards, but it is until the year of 1917 when the term robot is first used that comes from the Czech word "robota", which means servitude or forced labor. The beginnings of robotics are given by the year 1801 when Joseph Jacquard invents a programmable textile machine using punched cards, but it is until the year of 1917 when the term robot is first used that comes from the Czech word "robota", which means servitude or forced labor.

The characteristics of the kinematic model to be studied, is a haptic device Geomagic® Touch TM (OMNI PHANToM®) of Figure 8 provides an authentic three-dimensional navigation and feedback force and integrate the sense of touch in 3D modeling systems, as well as in commercial and research applications. This 3D Systems haptic device can accurately measure the 3D spatial position (along the X, Y and Z axes) and the orientation (turn, tilt and direction) of the hand pencil. It uses motors to create the forces of return in the hand of the user to simulate the touch and interaction with virtual objects, that is, it provides a feedback of force of 3 degrees of freedom (DOF) (3DSystems, 2013 and Silva, 2009, Vidrios- Serrano, et al., 2018, Yiannoutsou and Price, 2018).

Table 1 shows the technical specifications of the OMNI PHANToM haptic device and figure 1 shows the device. As you can see, it can be modeled kinematically as a manipulator robot, Almasi and Behzad, (2018).

Description	Characteristic
Work area	160An × 120Al × 70P mm
Range of movement	Movement of the hand with twist of the wrist
Nominal resolution	0.055mm
Maximum strength	3.3N
Force feedback	X and Z
Port interface	Ethernet conforming to RJ45

**Table 1** Geomatic® Touch device specifications



**Figure 1** Geomagic® TouchTM (OMNI PHANToM®)

A robot arm can be modeled as an articulated chain in open loop with rigid bodies (links) connected in series by revolute joints or prismatic driven by actuators. One end of the chain is attached to a fixed coordinate system at the base of the manipulator while the other end is free. For the control of the manipulators we want to know the spatial description of the free end with respect to the fixed reference coordinate system of the base (Spong & Vidyasagar, 1989, Schilling, 2000, Tsai, 1999).

The analytical study of the geometry of the manipulators with respect to a fixed reference coordinate system without considering the forces / moments that originate said movement is known as kinematic study (Barrientos, 1999, Fu, 1987). There are two problems to solve in terms of the kinematics of a robot arm; to the relationship that exists between the joint coordinates ( $\theta$ ) with the Cartesian coordinates ( $x$ ) and its orientation is known as direct kinematics, while the inverse function is known as inverse kinematics, as exemplified in Figure 2. The kinematics is divided into three: position, speed and acceleration.

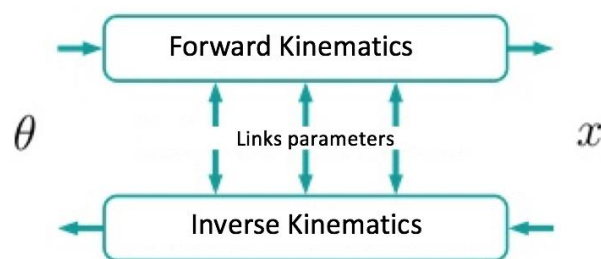


**Figure 2** Direct and inverse kinematic problem

### Kinematic position model

The problem of direct kinematics is reduced in finding the homogenous transformation matrix that relates the end of the manipulator to a reference system in the base of the device. The homogenous transformation matrix is composed of a rotation matrix (R), a position vector (P) Cartesian, a perspective vector (f) and the scale as shown in equation 1. By the year 1955 Denavit and Hartenberg creates an algorithm to find this matrix, which describes the spatial geometry of a robot arm with respect to a fixed coordinate system.

$$T = \begin{bmatrix} \mathbf{R}_{(3 \times 3)} & \mathbf{P}_{(3 \times 1)} \\ \mathbf{f}_{(1 \times 3)} & 1 \end{bmatrix} \quad (1)$$

#### a) Parameters of Denavit - Hartenberg

This method is based on determining four parameters:  $\theta_i$ ,  $\alpha_i$ ,  $d_i$  and  $a_i$ , related to the links  $i$  of the robot, to define the homogeneous transformation matrices of each link  ${}^{i-1}A_i$ , they are represented as a product of four basic transformations, as shown in equation 2, (Angeles, 1997, Fu, 1987, Kelly, 2003, Reyes, 2011).

$${}^{i-1}A_i = Rot_{z,\theta_i} Trans_{z,d_i} Trans_{x,a_i} Rot_{x,\alpha_i} \quad (2)$$

Where:

- $\theta_i$  The angle from the axis  $X_{sc_{i-1}}$  to  $X_{sc_i}$  measured around the axis  $Z_{sc_{i-1}}$
- $\alpha_i$  The angle between the axis  $Z_{sc_{i-1}}$  and  $Z_{sc_i}$ , measured around the axis  $X_{sc_i}$ .
- $d_i$  The distance along the axis  $Z_{sc_{i-1}}$  of the coordinate system  $O_{sc_{i-1}}$  to the intersection of  $X_{sc_i}$  and  $Z_{sc_{i-1}}$ .
- $a_i$  The distance along the axis  $X_{sc_i}$  of the coordinate system  $O_{sc_i}$  to the intersection of the axis  $X_{sc_i}$  and  $Z_{sc_{i-1}}$  to  $Z_{sc_i}$ .

The homogeneous transformation matrix proposed by Denavit and Hartenberg is shown in equation 3.

$${}^{i-1}A_i = \begin{bmatrix} \cos \theta_i & -\sin \theta_i \cos \alpha_i & \sin \theta_i \sin \alpha_i & a_i \cos \theta_i \\ \sin \theta_i & \cos \theta_i \cos \alpha_i & -\cos \theta_i \sin \alpha_i & a_i \sin \theta_i \\ 0 & \sin \alpha_i & \cos \alpha_i & d_i \\ 0 & 0 & 0 & 1 \end{bmatrix} \quad (3)$$

Figure 3 shows the assignment of the coordinate systems for the OMNI PHANToM® device according to the Denavit-Hartenberg algorithm, considering that its initial position where the angles  $\theta_1$ ,  $\theta_2$  and  $\theta_3$  are  $0^\circ$ .

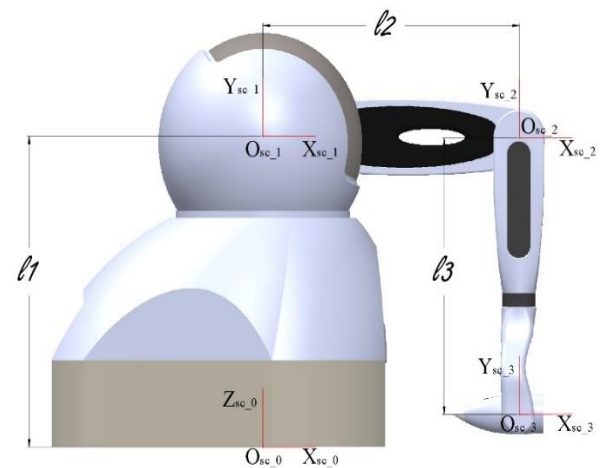


Figure 3 Assignment of coordinate systems

Table 2 shows the parameters of Denavit - Hartenberg for each link of the OMNI PHANToM®.

Joint	$\theta_i$	$\alpha_i$	$d_i$	$a_i$
1	$\theta_1$	$90^\circ$	$l_1$	0
2	$\theta_2$	$0^\circ$	0	$l_2$
3	$\theta_3 - 90^\circ$	$0^\circ$	0	$l_3$

Table 2 Parameters of Denavit – Hartenberg

The haptic device has a particularity in its link 2, because when it rotates the coordinate system  $\{O_{sc2}\}$  remains in the same orientation, which only undergoes translation. So the matrixes  ${}^{i-1}A_i$  for joints 1 and 3 are obtained according to equation 4, while for articulation 2 only a translation matrix is applied. For the purpose of simplifying the equations one has to  $\cos(\theta_i) = C\theta_i$  y  $\sin(\theta_i) = S\theta_i$  as well as using the trigonometric property  $\cos(\theta_3 - 90^\circ) = \sin(\theta_3)$  y  $\sin(\theta_3 - 90^\circ) = -\cos(\theta_3)$ .

$${}^0A_1 = \begin{bmatrix} C\theta_1 & 0 & S\theta_1 & 0 \\ S\theta_1 & 0 & -C\theta_1 & 0 \\ 0 & 1 & 0 & l_1 \\ 0 & 0 & 0 & 1 \end{bmatrix} \quad (4)$$

$${}^2A_3 = \begin{bmatrix} S\theta_3 & C\theta_3 & 0 & l_3 S\theta_3 \\ -C\theta_3 & S\theta_3 & 0 & -l_3 C\theta_3 \\ 0 & 1 & 1 & 0 \\ 0 & 0 & 0 & 1 \end{bmatrix}$$

While the translation matrix for joint 2 on the x axis is given by equation 5.

$${}^1A_2 = T_x = \begin{bmatrix} 1 & 0 & 0 & l_2 C\theta_2 \\ 0 & 1 & 0 & l_2 S\theta_2 \\ 0 & 0 & 1 & 0 \\ 0 & 0 & 0 & 1 \end{bmatrix} \quad (5)$$

The homogenous transformation matrix that relates the final end to the reference coordinate system results from the multiplication of the matrices of the equations 4 and 5,  $T = {}^0A_1 \cdot T_x \cdot {}^2A_3$ , where  $l_1 = l_2 = l_3 = l$ .

$$T = \begin{bmatrix} C\theta_1 & 0 & S\theta_1 & 0 \\ S\theta_1 & 0 & -C\theta_1 & 0 \\ 0 & 1 & 0 & l \\ 0 & 0 & 0 & 1 \end{bmatrix} \begin{bmatrix} 1 & 0 & 0 & l C\theta_2 \\ 0 & 1 & 0 & l S\theta_2 \\ 0 & 0 & 1 & 0 \\ 0 & 0 & 0 & 1 \end{bmatrix} {}^2A_3 \quad (6)$$

$$= \begin{bmatrix} C\theta_1 & 0 & S\theta_1 & l C\theta_1 C\theta_2 \\ S\theta_1 & 0 & -C\theta_1 & l S\theta_1 C\theta_2 \\ 0 & 1 & 0 & l S\theta_2 + l \\ 0 & 0 & 0 & 1 \end{bmatrix} \begin{bmatrix} S\theta_3 & C\theta_3 & 0 & l S\theta_3 \\ -C\theta_3 & S\theta_3 & 0 & -l C\theta_3 \\ 0 & 1 & 1 & 0 \\ 0 & 0 & 0 & 1 \end{bmatrix}$$

Developing equation 6, you have

$$T = \begin{bmatrix} C\theta_1 S\theta_3 & C\theta_1 C\theta_3 & S\theta_1 & l(C\theta_1 S\theta_3 + C\theta_1 C\theta_2) \\ S\theta_1 S\theta_3 & S\theta_1 C\theta_3 & -C\theta_1 & l(S\theta_1 S\theta_3 + S\theta_1 C\theta_2) \\ -C\theta_3 & S\theta_3 & 0 & l(-C\theta_3 + S\theta_2 + 1) \\ 0 & 0 & 0 & 1 \end{bmatrix} \quad (7)$$

From the equation 7 we extract the position vector  $P_{3 \times 1}$  that solves the direct kinematic problem of position, and we obtain the direct kinematics, as shown in equation 8.

$$\begin{aligned} x &= l(C\theta_1 S\theta_3 + C\theta_1 C\theta_2) \\ y &= l(S\theta_1 S\theta_3 + S\theta_1 C\theta_2) \\ z &= l(-C\theta_3 + S\theta_2 + 1) \end{aligned} \quad (8)$$

### Inverse kinematic position model

One of the most used methods to solve the inverse kinematic problem in manipulators with few degrees of freedom is without doubt the **geometric**.

Its main characteristic is based on finding a sufficient number of geometric relationships (mainly triangles) in which the Cartesian coordinates of the robot end  $P(X_{sc0}, Y_{sc0}, Z_{sc0})$ , its joint coordinates and the dimensions of its links are related to each other (Craig, 2003, Paredes, 2018, Reyes, 2012, Siciliano, 2009, Spong & Vidyasagar, 1989).

Figure 4 shows a top view of OMNI PHANToM®, projecting the point  $P(X_{sc0}, Y_{sc0}, Z_{sc0})$  on the plane  $X_{sc0} Y_{sc0}$ , a right triangle is formed that allows finding the value of  $\theta_1$ .

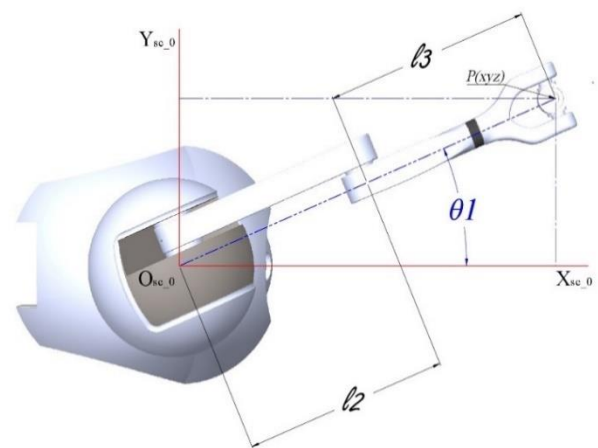
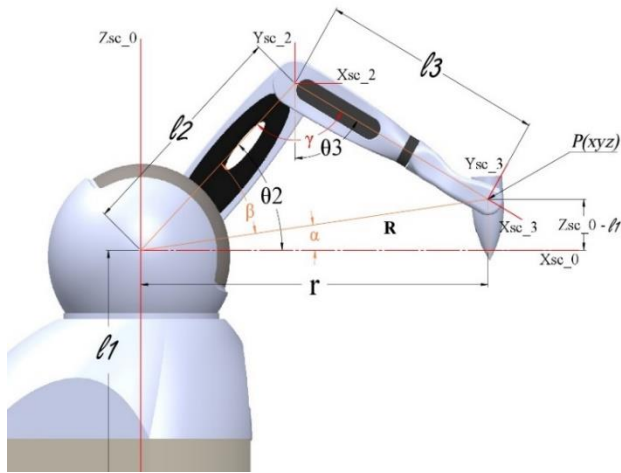


Figure 4 Top view to get the value of  $\theta_1$

Applying trigonometric properties we have equation 9, which represents the value of  $\theta_1$ .

$$\theta_1 = \arctan\left(\frac{Y_{sc0}}{X_{sc0}}\right) \quad (9)$$

A side view of the device is made as shown in figure 5, where only links 2 and 3 that are in the plane are considered.  $X_{sc0} Z_{sc0}$ . Due to the mechanical configuration of the haptic device it is analyzed in the elbow configuration above that observed in the figure. The value  $\theta_2$  this given by the value of the auxiliary angles as is the case of  $\alpha$  and  $\beta$ .



**Figure 5** Side view for obtaining angles  $\theta_2$  and  $\theta_3$

The value of  $\alpha$  is obtained from the right triangle formed by the vectors  $r$ ,  $R$  and  $Z_{sc_0} - l_1$ , where  $r$  is the vector  $P(X_{sc_0}, Y_{sc_0}, Z_{sc_0})$  proyectado sobre el plano  $X_{sc_0} Y_{sc_0}$  from figure 3 and they are obtained by means of equation 10.

$$r = \sqrt{X_{sc_0}^2 + Y_{sc_0}^2} \quad (10)$$

The vector  $R$  of equation 11 is the result of the point  $P(X_{sc_0}, Y_{sc_0}, Z_{sc_0})$  with the origin  $Z_{sc_0} - l_1$ . Also remember that  $l_1 = l_2 = l_3 = l$

$$R = \sqrt{r^2 + (Z_{sc_0} - l)^2} \quad (11)$$

applying trigonometric identities we obtain the value of  $\alpha$

$$\alpha = \arctan\left(\frac{Z_{sc_0} - l}{r}\right) \quad (12)$$

For the angle  $\beta$  part of the triangle formed in orange and by law of the cosines is equation 13.

$$\beta = \arccos\left(\frac{R}{2l}\right) \quad (13)$$

The angle  $\theta_2$  of equation 14 is the sum of the angles  $\alpha$  and  $\beta$  of equations 12 and 13 respectively.

$$\theta_2 = \alpha + \beta \quad (14)$$

The angle  $\theta_3$  is obtained through the auxiliary angle  $\gamma$ , the value of  $\theta_2$  in equation 14 and the  $90^\circ$  between the negative axis  $Y_{sc_2}$  and the positive axis  $X_{sc_2}$ , as shown in Equation 15.

$$\theta_3 = \gamma + \theta_2 - 90^\circ \quad (15)$$

where  $\gamma$  is obtained by equation 16

$$\gamma = \arccos\left(\frac{2l^2 - R^2}{2l^2}\right) \quad (16)$$

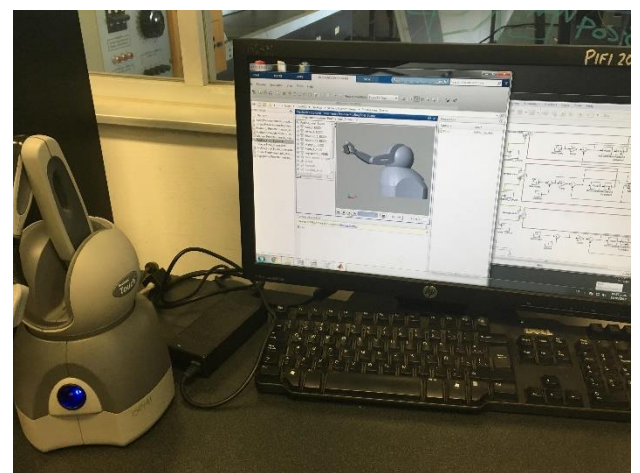
## Experimental results

### a) Experimental team

For the validation of the kinematic model, a computer used for the development of this project whose characteristics are shown in table 3, and an OmniPhantom haptic device, as shown in figure 6, is used.

First name	Characteristic
Brand	HP Brand
Model	Model xw6600 Workstation
Intel processor	Intel ® Xeon ® Processor CPU E5420 @ 2.50 GHz
Installed memory (RAM)	8.00 GB
Type of system	64-bit operating system
Windows edition	Windows 7 Ultimate

**Table 3** Computing equipment specifications

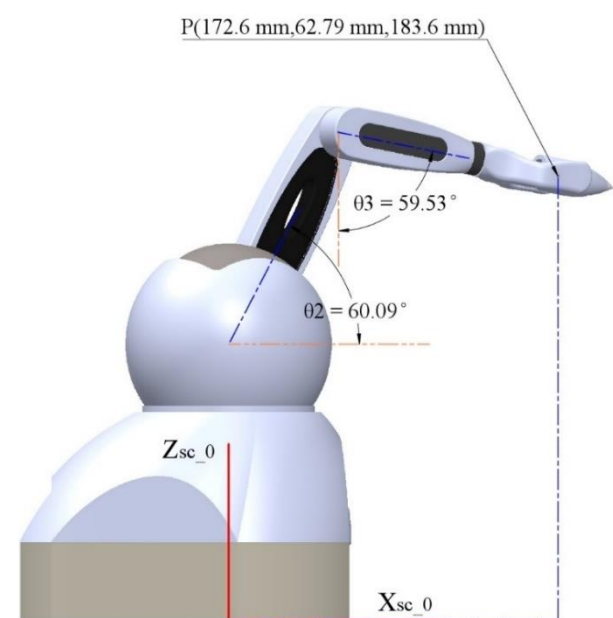
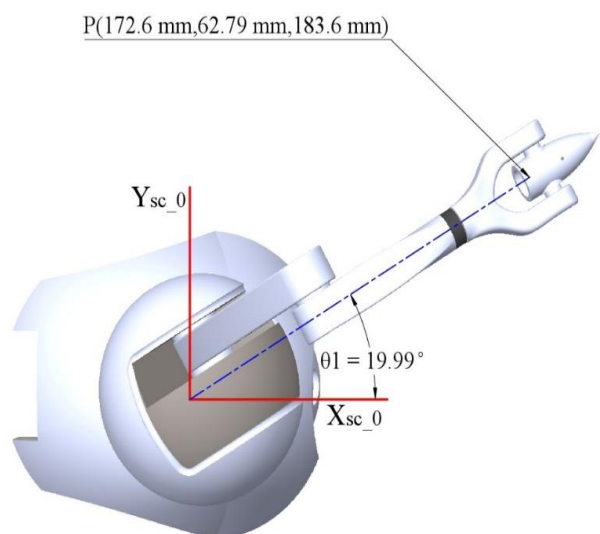


**Figure 6** Experimental team

### b) Forward Kinematics

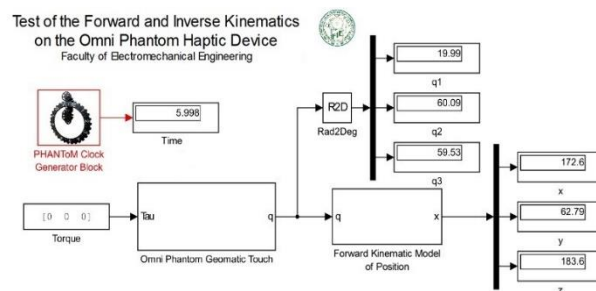
The experimental validation of equation 8 representing the Cartesian position of the final effector projected in the coordinate system  $O_{sc_0}$  is shown in figure 7, where the angular values are assigned to each of the joints:  $\theta_1 = 19.19^\circ$ ,  $\theta_2 = 60.09^\circ$  and  $\theta_3 = 59.53^\circ$ . Where it is appreciated that the Cartesian position is  $P(172.6mm, 62.79mm, 183.6mm)$ .



(a) Plane projection  $X_{sc_0}Z_{sc_0}$ (b) Plane projection  $X_{sc_0}Y_{sc_0}$ **Figure 7** Validation of the direct kinematics of the OMNI PHANToM®

PHANSIM is a tool for Simulink of the haptic devices of Sensable, this tool is for academic purposes and developed for the control of robot movement and teleoperation. Traditionally, to use these devices, it is necessary to generate codes in C / C++ using the OpenHaptics® libraries (SDK), which are provided by the manufacturer. With the use of this tool the use of the devices is facilitated.

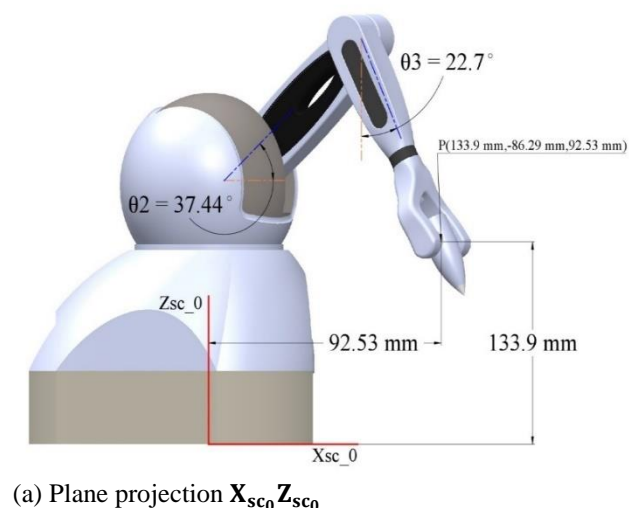
The OMNI PHANToM® device is brought to the aforementioned angular position to validate the Cartesian position, with the use of the PHANSIM library in Matlab's Simulink the interface shown in figure 8 is made.

**Figure 8** Validation of the OMNI PHANToM® direct kinematic model in Simulink

To allow the free movement of the device, a zero torque vector is sent to it, in the second block from left to right, the reading of the angular position of the device is read to later enter the block that calculates the direct kinematics, in which it is checked that the values of the Cartesian position coincide with those of the point  $P(X_{sc_0}, Y_{sc_0}, Z_{sc_0})$  shown in figure 7.

### b) Inverse position kinematics

For the validation of the inverse kinematic position model, the values of  $X_{sc_0} = 133.9 \text{ mm}$ ,  $Y_{sc_0} = -86.29 \text{ mm}$  and  $Z_{sc_0} = 92.53 \text{ mm}$  of the final effector with respect to the coordinate system  $O_{sc_0}$ , with the help of the model made in SolidWorks the values that the angles must take are verified  $\theta_1$ ,  $\theta_2$  y  $\theta_3$ , as shown in figure 9.

(a) Plane projection  $X_{sc_0}Z_{sc_0}$

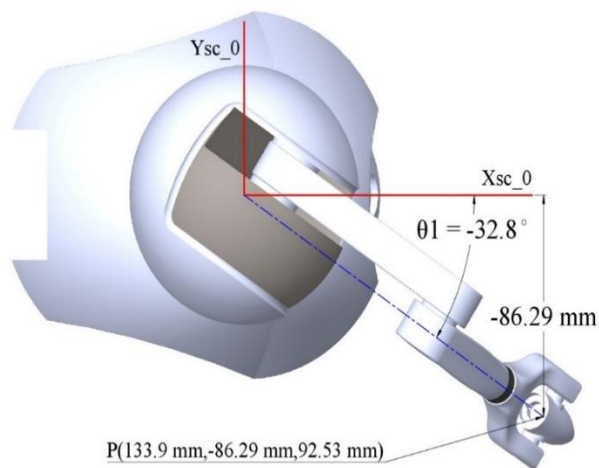
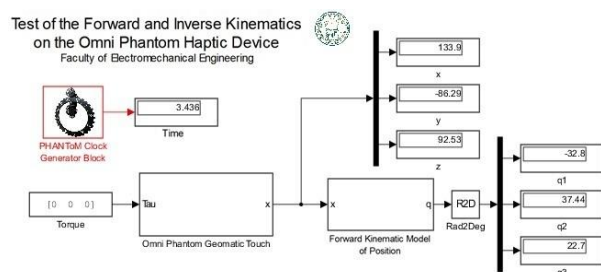
(b) Plane projection  $X_{sc_0}Z_{sc_0}$ **Figure 9** Validation of the inverse kinematics of OMNI PHANToM®

Figure 10 shows the experimental validation with the OMNI PHANToM® through the PHANSIM library in which it is verified that for the given position the angles are:  $\theta_1 = -32.8^\circ$ ,  $\theta_2 = 37.44^\circ$  and  $\theta_3 = 22.6^\circ$ .

**Figure 10** Validation of the inverse kinematic model of the OMNI PHANToM® in Simulink

## Conclusions

In the present work, the direct and inverse kinematic model of the OMNI PHANToM® haptic device is shown, which is essential for the modeling and simulation of mechanical systems. A simple mathematical analysis is presented to facilitate the reader. A three-dimensional model is developed on the SolidWorks platform for the validation and understanding of the behavior of direct and inverse kinematics.

Through the use of the PHANSIM library, the experimental validation is carried out in the Matlab Simulink platform, where it is appreciated that the proposed model is correct.

The experimental results obtained from the OMNI PHANToM® are correct, that is to say, for the direct kinematics several angles were introduced and the Cartesian position is obtained correctly, the same is done for the reverse kinematics validation, the position is introduced of the end effector and the angles of each article of OMNI PHANToM® are obtained, so it is concluded that the mathematical analysis of the direct and inverse kinematics are correct. For future work in the area of control of robot manipulators the dynamic model is developed.

## Acknowledgement

The authors thank the Faculty of Electromechanical Engineering of the University of Colima for all the facilities granted to carry out this project and the SES-PRODEP for supporting the project of the Academic Body UCOL-CA-21 with key number IDCA-691 "Diagnosis and Re-Enabling Superior Member with a Robot".

## References

Almasi, O. N., Khooban, M. H., & Behzad, H. (2018). Non-linear MIMO identification of a Phantom Omni using LS-SVR with a hybrid model selection. IET Science, Measurement & Technology.

Angeles, Jorge. (1997). Fundamentals of robotic mechanical systems: theory, methods and algorithms. USA: Springer.

Barrientos, Antonio, Peñín, Luis Felipe, Carlos Balaguer & Rafael Aracil. (1999). Fundamentos de Robótica. España: McGraw Hill.

Craig, John J. (2003). Introduction to robotics: mechanical and control. (Third edition). USA: Prentice Hall.

Fu, K.S., R. C. González, & C. S. G. Lee. (1987). Robotics: control, sensing, vision and intelligence. USA: McGraw Hill.

Kelly, Rafael, Santibáñez, Víctor. (2003). Control de movimiento de Robots Manipuladores. España. Pearson & Prentice Hall.

Paredes Anchatipán, A. (2018). Teleoperación de un brazo robot Kinova MICO2 a través de un dispositivo Omni Bundle. Tesis Maestría. Universidad de Alicante.

Reyes, Fernando. (2011). Robótica Control de Robots Manipuladores. AlphaOmega.

Reyes, Fernando. (2012). Matlab Aplicado a Robótica y Mecatrónica. AlphaOmega.

Schilling, Robert J. (2000). Fundamentals of robotics: analysis & control. USA: Book News Inc.

Siciliano, Bruno, Sciavicco, L., Villani, L., Oriolo, G. (2009). Robotics Modelling, Planning and Control. London. Springer-Verlag.

Silva A, O, V y J. (2009). Phantom omni haptic device: Kinematic and manipulability. Electronics, Robotics and Automotive Mechanics Conference (CERMA).

Spong, Mark W. & M. Vidyasagar. (1989). Robot dynamics and control. USA: John Wiley & Sons.

Tsai Lung-Wen. (1999). Robot Analysis: The mechanic of Serial and Parallel Manipulators. Editorial: John Wiley & Sons, Inc. ISBN 0-471-32593-7.

Vidrios-Serrano, C. A., Maldonado-Fregoso, B. R., Bonilla-Gutiérrez, I., Mendoza-Gutiérrez, M. O., & González-Galván, E. J. (2018). Integración de un Sistema Robótico de Terapia Ocupacional para Extremidades Superiores con Estimulación Visual/Táctil de Los Pacientes. Revista mexicana de ingeniería biomédica, 39(2), 144-164.

Yiannoutsou, N., Johnson, R., & Price, S. (2018). Exploring how children interact with 3D shapes using haptic technologies. In Proceedings of the 17th ACM Conference on Interaction Design and Children (pp. 533-538). ACM 3DSystems. Geomagic ® touch device guide. 2013.